# Cross-Shore Currents in the Surf Zone: Rips or Undertow?

Authors: Aagaard, Troels, and Vinther, Niels

Source: Journal of Coastal Research, 2008(243) : 561-570

Published By: Coastal Education and Research Foundation

URL: https://doi.org/10.2112/04-0357.1

| Journal of Coastal Research | 24 | 3 | 561–570 | West Palm Beach, Florida | May 2008 |
|---|---|---|---|---|---|

# Cross-Shore Currents in the Surf Zone: Rips or Undertow?

**Troels Aagaard and Niels Vinther**

Institute of Geography
University of Copenhagen
Øster Voldgade 10
DK-1350, Copenhagen K
Denmark
taa@geogr.ku.dk

**ABSTRACT**

AAGAARD, T. and VINTHER, N., 2008. Cross-shore currents in the surf zone: Rips or undertow? *Journal of Coastal Research,* 24(3), 561–570. West Palm Beach (Florida), ISSN 0749-0208.

Although the dynamics and kinematics of various types of mean cross-shore current flows in the surf zone (undertow and rip currents) are fairly well understood, the causes for transitions occurring between these two types of mean circulation patterns remain obscure. On longshore barred beaches, such transitions involve the formation, degeneration, or both of rip channels. In this paper, field evidence is presented to suggest that transitions between undertow and rip current (cell) circulations could depend on the magnitude of the wave-induced onshore mass transport across a longshore bar, rip channel spacing, and trough cross-sectional area. The results are based on data obtained from four field experiments on the Danish and Dutch North Sea coasts, which encompassed a range of incident wave energy conditions. Two of the data sets demonstrate transitions between cell and undertow circulations. Calculated onshore-directed mass transports in the two circulation types were plotted against $A_t/y_r$, where $A_t$ is trough cross-sectional area and $y_r$ is longshore distance from the measurement position to a rip channel. The two types of circulation are separated in parameter space by a straight line with a slope of 1 (m/s). The observations support a model proposed previously, in which optimum rip spacings exist that depend on the balance between onshore discharge and longshore pressure gradients caused by irregular bar bathymetry. This simple morphodynamic model indicates that both hydrodynamic conditions and existing bathymetry are critical in determining the type of mean current circulation.

**ADDITIONAL INDEX WORDS:** *Cell circulation, mean currents, beach morphodynamics, beach processes, Skallingen, Egmond.*

## INTRODUCTION

Rip currents and undertows are the two major types of offshore-directed mean flows which exist in surf zones. Both mean current systems are driven by radiation stress and set-up gradients caused by wave breaking and they are fed by the onshore mass transport of water supplied by the (breaking) incident waves (MASSELINK and BLACK, 1995; SVENDSEN, 1984).

The undertow is defined as a laterally homogeneous current flowing offshore near the sea bed (*e.g.,* GREENWOOD and OSBORNE, 1990). This mean current circulation can be perceived as a vertically segregated flow consisting of the wave-driven onshore mass transport in the upper layers of the water column (between wave crest and wave trough) and the offshore-directed undertow near the bed (SVENDSEN, 1984). Undertows typically occur during high-energy wave conditions and in association with two-dimensional nearshore bathymetries consisting of planar slopes or quasi-linear bars and troughs, corresponding to the dissipative beach state (*cf.* WRIGHT and SHORT, 1984). Mean offshore current speeds can be up to about 0.5 m/s (*e.g.,* GARCEZ FARIA *et al.,* 2000; HAINES and SALLENGER, 1994), and the undertow potentially carries large amounts of sediment seaward. Hence, in many cases, undertow contributes to nearshore bar formation (AAGAARD, NIELSEN, and GREENWOOD, 1998; DYHR-NIELSEN and SØRENSEN, 1970; HOLMAN and SALLENGER, 1993).

Rip currents are laterally confined, jet-like currents that are also directed seaward from the surf zone (BOWEN, 1969; MCKENZIE, 1958; SHEPARD and INMAN, 1950). Because of their narrow, horizontally constricted nature and the occasionally large flow velocities, rip currents have drawn the attention of many beach users. Rip currents depend on the existence of longshore pressure (set-up) gradients caused by alongshore variations in radiation stress (KOMAR, 1998). Such longshore radiation stress gradients are typically caused by longshore variability in wave breaking intensity because of irregular bar topography (SONU, 1972). Consequently, rip currents are often generated in the more moderate-energy intermediate beach states which exhibit three-dimensional sinuous, crescentic, or transverse bar patterns (*cf.* WRIGHT and SHORT, 1984).

On barred beaches and with normally incident waves, rip cells consist of longshore-directed rip feeder currents, located in troughs landward of bars, and seaward-directed rip currents located in depressions or gaps along the bar structure (rip channels). The circulation cells are completed by onshore-

*DOI: 10.2112/04-0357.1 received 16 January 2005; accepted in revision 9 March 2006.*

This study was funded jointly by the EU CoastView-project (contract EVK3-CT-2001-00054) and the Danish Technical Sciences Research Council (grant 9901287).

directed mean currents across bars between rip channels (AAGAARD, NIELSEN, and GREENWOOD, 1998; FALQUES, MONTOTO, and IRANZO, 1996; KLEIN and SCHUTTELAARS, 2005; KROON and DEBOER, 2001); these onshore flows are generally almost uniform in the vertical (GRANT, 1999; HALLER, DALRYMPLE, and SVENDSEN, 2002; MACMAHAN *et al.,* 2005; MACMAHAN, THORNTON, and RENIERS, 2006). Hence, the mean current (cell) circulation is horizontally segregated, and rip circulations tend to result in landward-migrating bars between rip channels (AAGAARD, NIELSEN, and GREENWOOD, 1998; SHORT, 1985; WRIGHT and SHORT, 1984). Rip currents are often spaced at intervals of 50–1000 m, but the causes for the quasi-regular spacings are not well understood (HOLMAN *et al.,* 2006; HUNTLEY and SHORT, 1992). The rip channels might migrate alongshore, driven by a longshore current, but rip channels on the Dutch North Sea coast have also been observed stationary for several months (AARNINKHOF *et al.,* 2003). Mean rip current velocities are typically on the order of 0.2–0.7 m/s (AAGAARD, GREENWOOD, and NIELSEN, 1997; BOWMAN *et al.,* 1988; MACMAHAN, THORNTON, and RENIERS, 2006; SONU, 1972), but they can attain speeds of 1 m/s or more (BRANDER and SHORT, 2000; SHEPARD and INMAN, 1950; SHORT and HOGAN, 1994). In the special case of transverse bar morphology, rip channels are deep and narrow, rip feeders are short or lacking, and a large part of the water mass feeding the rip current is probably caused by side drainage off the bars (BRANDER, 1999; MACMAHAN *et al.,* 2005).

Field data from active rips are scarce because of the difficulties with installing instruments under conditions with strong mean currents and because of the potentially varying spatial position of the channels. Because of the scarcity of field data, numerical modelling of rip currents has become an increasingly used tool to analyse and quantify cell circulation (*e.g.,* DAMGAARD *et al.,* 2002; DRØNEN *et al.,* 2002; HAAS *et al.,* 2003; HALLER, DALRYMPLE, and SVENDSEN, 2002). Modelling results indicate that although the kinematics and dynamics of rip cell circulations can be predicted fairly well, the causes for transitions occurring between undertow and rip cell circulations and the ensuing generation and decay of rip channels, as well as the factors determining rip spacing, are less well understood.

In a recent modelling study, DEIGAARD *et al.* (1999) suggested that optimum rip current spacings exist; these spacings depend on the cross-shore discharge of water across the bar. Because of differences in the wave breaker pattern caused by irregular bar topography, the cross-shore discharge in their model varies harmonically in the alongshore direction with a wavelength of $\lambda$ (determined by the bar topography) and an amplitude that varies nonlinearly with wave height across the bar. With a given onshore discharge, and in a situation with very large $\lambda$, longshore set-up gradients become small and incapable of overcoming flow resistance in the trough to force the (rip feeder) discharge alongshore towards the rip channel. Consequently, an undertow develops instead of a rip circulation. For very short $\lambda$, the inertia of the water discharged onshore reduces longshore set-up gradients that should again result in undertow circulation. In between these two limiting cases, an optimum (range of) rip current spacing(s) exists. With increased wave heights across the bar, discharge amplitude increases, longshore set-up gradients increase, the preferred $\lambda$ (rip spacing) increases, and *vice versa.* Hence, in this numerical model, rip spacing depends on the balance between onshore discharge and longshore set-up gradient. DEIGAARD *et al.* (1999) demonstrated that this balance also involves the cross-sectional area of the trough landward of the bar. Because a balance exists between longshore set-up gradient and flow resistance in the trough, larger trough areas improve hydraulic efficiency and longshore drainage, and for a given onshore discharge, they obtained a linear relationship between rip spacing and the square root of the trough area.

The aim of this study is to use field data to test the hypothesis that a critical threshold exists that determines the type of mean current circulation. The threshold involves the ratio between onshore wave-induced mass transport across the nearshore bar crest ($Q$), the cross-sectional area of the landward trough ($A_t$), and the distance between rip channels, $\lambda$. If onshore mass transport exceeds this threshold, an undertow should be generated. On the other hand, if the trough volume is sufficiently large relative to onshore discharge, there should be a tendency for rip cell circulation.

Field data from four experiments on two long, straight sandy beaches with micro/mesotidal conditions and multiple longshore bars were analysed. Such settings are typical for the wind wave–dominated coastlines of northern Europe, and both beaches exhibit frequent switches between rip cell and undertow circulations.

## STUDY SITES

### Skallingen

This study site is located on the west coast of a barrier spit on the Danish North Sea coast. The shoreline is slightly concave but without interruptions over an alongshore distance of 12 km. The mean annual offshore significant wave height is 1.0 m, and wave periods are typically 4–6 seconds. During intense onshore storms, however, significant wave heights exceed 4 m in deep water with peak spectral wave periods up to 13 seconds. Tides are semidiurnal, with a mean range of 1.5 m (1.3 m at neaps and 1.8 m at springs). The sand on the west coast of Skallingen has a mean grain size of 160–230 $\mu$m, and the nearshore gradient ($\beta$) is about 0.007, steepening to 0.02–0.03 in the intertidal zone (Figure 1). Generally, two or three subtidal bars and an intertidal bar are present. These bars are quasi-linear, and the intertidal as well as the inner subtidal bars are often dissected by rip channels, typically spaced at 200–350 m.

### Egmond

The Egmond field site is located on the Dutch coast about 1.5 km south of the town of Egmond aan Zee. Like Skallingen, it is a wave-dominated mixed-energy coast (DAVIS and HAYES, 1984) with a mean tidal range of 1.65 m (1.4–2.1 m). The mean annual significant offshore wave height is $\sim$1.2 m with wave periods of 5 seconds. The shoreface is somewhat steeper than at Skallingen, $\beta \approx 0.0135$ (Figure 1). It is a

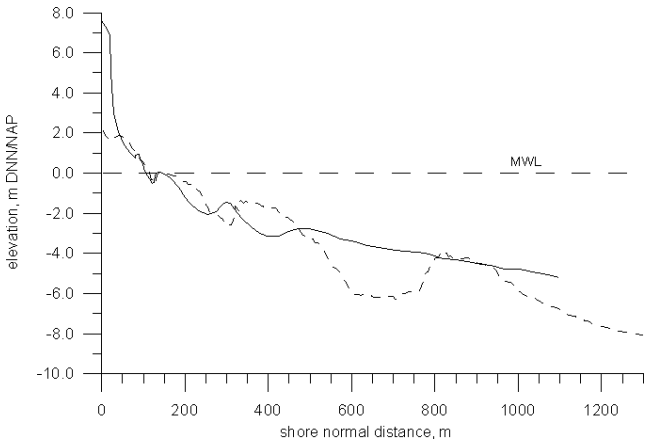


Figure 1. Cross-shore shoreface profiles from Skallingen (solid) and Egmond (dashed; courtesy of A. Kroon).

double-barred system with an additional intertidal bar, but the troughs are significantly deeper and the bars are steeper and larger at Egmond than at Skallingen. The subtidal bars are typically sinuous or exhibit crescentic shapes. The intertidal bars are frequently dissected by rip channels, with a spacing of 40–500 m (KROON *et al.,* 2003), and the inner subtidal bar is also generally rhythmic with rip currents and channels. The mean grain size of the beach sediment is 250–300 μm, with an offshore fining to 200 μm in the outer nearshore zone.

## METHODS AND DATA ANALYSIS

The analysis is based on data sets obtained from four field experiments, three of which were conducted at Skallingen in 1995 (SK95), 2000 (SK00), and 2002 (SK02), and the final experiment was conducted at Egmond in 2002 (EG02). The field experiments included measurements of hydrodynamics and sediment transport as well as surveys of nearshore and intertidal bathymetry (AAGAARD, 2002; AAGAARD *et al.,* 2005).

The hydrodynamic data were collected from cross-shore instrument arrays of three to six stations, but in this paper, only results from the stations on inner subtidal or intertidal bar crests are presented. Figure 2 illustrates the extent and position of the arrays. The instrument transects were placed across bar crests midway between rip channels (SK95, SK02, EG02). During SK00, instruments were placed across bars as well as along rip feeders and in a rip channel (Figure 3).

Measurements of waves and currents were obtained in instrument runs of 45 minutes duration, with a sampling frequency of 10 Hz, except at SK95, when runs of 34 minutes duration with a sampling frequency of 4 Hz were collected. Mean currents and orbital velocities were generally measured with Marsh-McBirney OEM512 biaxial electromagnetic current meters deployed ~0.2 m above the seabed. Mean current speeds below 0.05 m/s were excluded from the present analyses because of the conservative limit of instrument errors (GUZA, CLIFTON, and REZVANI, 1988). During SK02

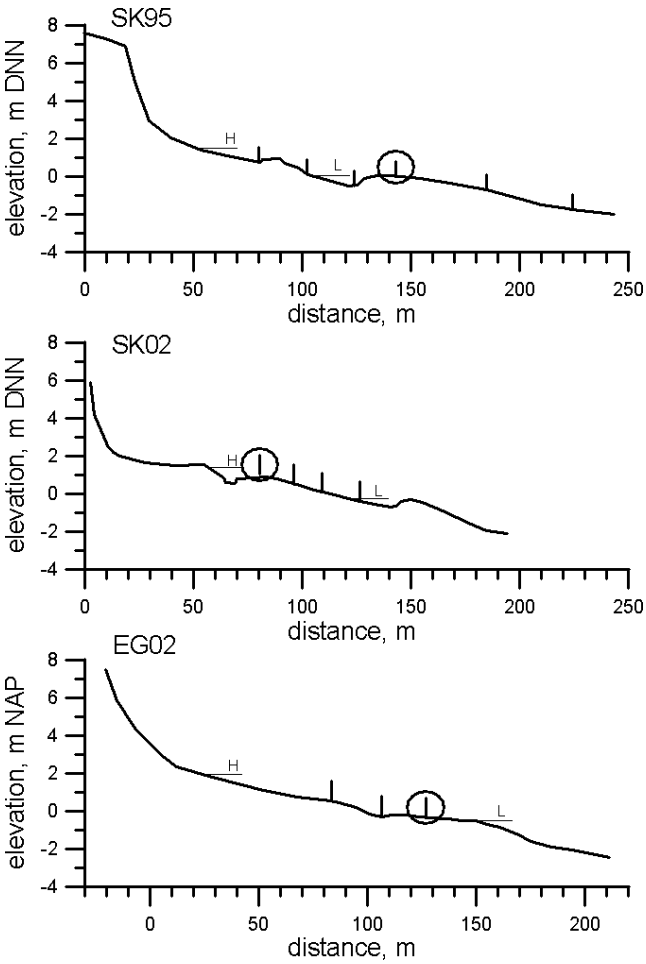


Figure 2. Cross-shore profiles of the upper shoreface during the experiments of SK95, SK02, and EG02. The positions of instrument stations are indicated by the vertical bars. Only data from bar crests/upper seaward bar slopes (indicated by circles) are used here. The thin horizontal bars and the letters H and L indicate the high and low mean water levels, respectively, during the experiments.

and EG02, fluid velocities were also recorded with Sontek 10 MHz ADV's. Wave heights and mean water surface elevations at the different stations were measured with pressure transducers (Viatran model 240), which were mounted on most stations; if pressure sensors were lacking at a particular station, incident wave heights were estimated from measured orbital velocities as $H_{rms} = \sqrt{8}(\langle\sigma^2\rangle h/g)^{0.5}$ (THORNTON and GUZA, 1989), where $\langle\sigma^2\rangle$ is the total time-averaged velocity variance, $h$ is mean water depth, and $g$ is the acceleration of gravity. Before conversion from orbital velocity to wave height, the velocity records were high-pass filtered to avoid contributions from low-frequency wave motions in the wave height estimates. Water levels were corrected for barometric pressure with pressure data from nearby meteorological stations. Water depths, $h$, were estimated with the use of water levels and topographic surveys. Offshore wave records at Skallingen were obtained from a pressure sensor located at

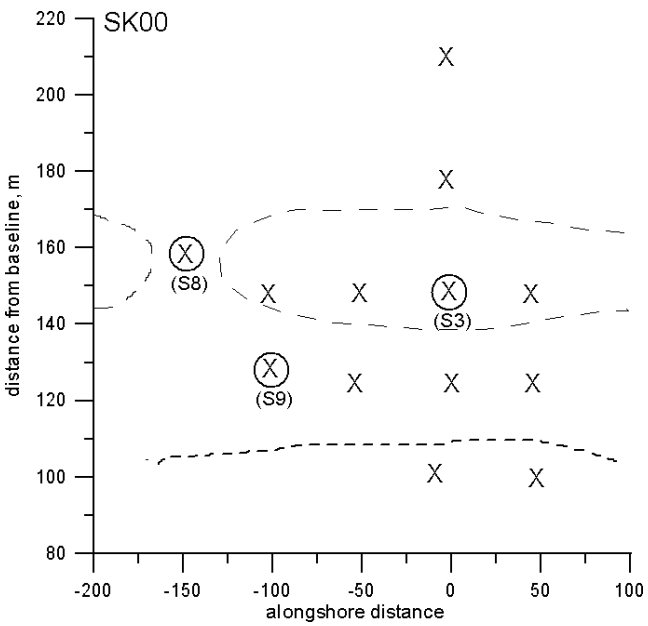


Figure 3. Plan view of the instrument array during the SK00 experiment. Long dashes approximately outline the intertidal bar crest, and the short dashes show the mean shoreline position during the experiment. Numbers and circles indicate stations from which data have been used in this paper.

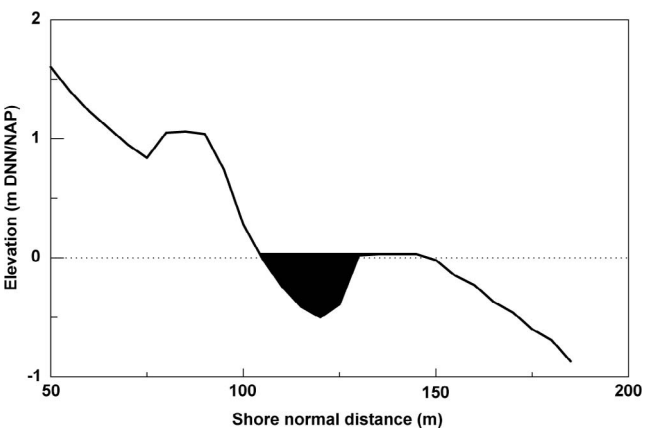


Figure 4. Sketch illustrating the calculation of trough cross-sectional area. This trough area (shaded) is estimated between bar crest level and the corresponding level at a position landward of the bar.

a water depth of 6–7 m; at Egmond, offshore data from a Waverider buoy at a depth of 21 m were used.

Onshore discharge across a longshore bar ($Q$, $m^3\ s^{-1}\ m^{-1}$) was estimated from wave parameters obtained close to the breakpoint on the seaward slope of that bar. The discharge was calculated as the sum of Stokes drift ($Q_{drift}$) due to asymmetries in the wave orbits and mass transport from the surface roller ($Q_{roller}$),

$$Q = Q_{drift} + Q_{roller} = \frac{CB_0H_{rms}^2}{h} + \frac{A}{T} \quad (1)$$

(Fredsøe and Deigaard, 1992; Svendsen, 1984), where $C$ ($= (gh)^{0.5}$) is shallow water wave phase speed, $B_0$ ($\approx 0.125$) is a wave shape factor, $A$ ($= 0.9H^2$) is the area of the surface roller, and $T$ is incident wave period.

Because instruments were not installed in rip channels except at SK00, the presence or absence of rip cell circulation was determined by three criteria: (1) Visual observations of the flow pattern at times of recording, (2) the presence or absence of rip channels, verified at low tide, and (3) the direction of the mean current at bar crests at times of recording. Offshore-directed flows near the bed at bar crests signify a dominance of undertow, whereas onshore-directed mean flows (at bar crests) are associated with rip circulations. As discussed above, a number of field and laboratory experiments have demonstrated almost vertically uniform onshore-directed mean flows across bar crests (in conjunction with offshore flows in rip channels) at times of cell circulation. Such onshore flows near the bed are probably due in part to the strongly vertically mixed water column under intensely breaking waves and bores in shallow water (Longo, Petti, and Losada, 2002; Svendsen, 1987).

Topographic surveys were conducted in transects that were offset from the instrument transect by about 5 m. Steel rods with a cross-shore spacing of 2–5 m were jetted into the bed, and the distance from the top of the rods to the sand surface was measured at each low tide, after the top of the rods had been surveyed relative to a known datum with the use of a total station. By this method, a rapid and quite accurate survey of the profile line is feasible (Aagaard, Nielsen, and Greenwood, 1998). These surveys were supplemented by area surveys spanning the bar and adjacent rip channels (if present) with total stations. The distance to (downdrift) rip channels ($y_r = \frac{1}{2}\lambda$), which affects the set-up gradient for a given longshore bar shape (Deigaard *et al.,* 1999), was determined on the basis of the area surveys and distance measurements in the field. The cross-sectional area of the trough landward of the bars ($A_t$) was determined from the morphological surveys and calculated as the area between the level of the bar crest and the sand bed (see Figure 4). $A_t$ was determined by linear interpolation between consecutive surveys to obtain a trough area for each hydrodynamic data record. Note that trough area does not extend to the mean water surface because it is the wetted perimeter that is important to flow resistance. Furthermore, use of the mean water surface as the upper boundary introduces more ambiguity into the determination of trough area because intertidal bars and runnels, as well as other irregularities, often existed landward of a subtidal bar. In such cases, determination of trough area with mean water level as the upper boundary would have been based on subjective choices and sporadic observations of whether intertidal bars and runnels were part of the main circulation system or whether secondary circulations were generated across the intertidal systems. Finally, tests with run-averaged mean water levels as the upper trough boundary resulted in more data scatter.

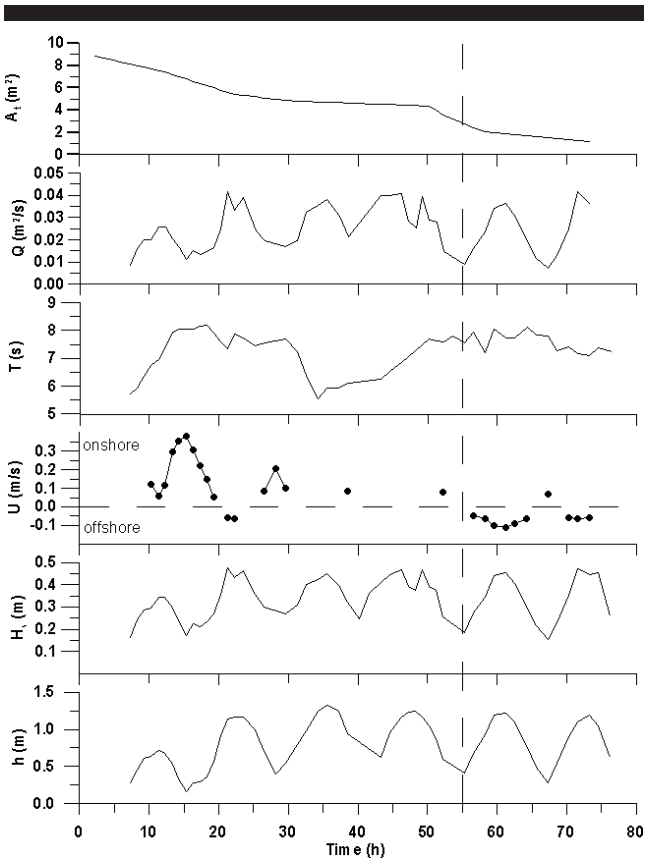


Figure 5. Hydrodynamic conditions at the inner bar crest during the SK95 experiment. The panels illustrate (bottom to top): mean water depth, significant wave height, and mean cross-shore current velocity, all at the crest of the inner bar; incident wave period at the seaward limit of the instrument array; calculated onshore discharge across the inner bar; and finally, cross-sectional area of the trough landward of the bar. All tidal cycles, except for the first, had almost similar wave heights/periods and high/low mean water levels. Mean current velocities were mainly onshore-directed during the first four tidal cycles, but offshore after hour 55 (marked by a dashed vertical line) when the trough infilled rapidly.

## RESULTS

### SK95

The SK95 experiment exhibited a transition from rip cell to undertow circulation. Measurements were obtained from the crest of the inner subtidal bar, and the instrument transect crossed the bar halfway between two rip channels, spaced 180 m on either side of the transect ($\lambda = 360$ m). The data set used here (Figure 5) spanned six tidal cycles, with moderate wave energy levels and offshore significant wave heights up to 1.86 m. During the first tidal cycle, the maximum water depth over the bar crest was 0.70 m, but during the ensuing five tidal cycles, water levels increased, and high tide water depths over the bar crest were 1.17–1.33 m. Significant wave heights were strongly dependent on water depth, with the largest wave heights and onshore discharges occurring at high tide (Figure 5). Initially, the mean current over the bar was onshore-directed, indicating a rip circulation. Current speeds peaked at low tide, up to 0.38 m/s during the first tidal cycle when the depth of water over the bar was small. Onshore current speeds decreased over the next three tidal cycles. The current transported sediment landward across the bar, which resulted in an onshore bar migration (AAGAARD, NIELSEN, and GREENWOOD, 1998) and a decrease in trough area from about 8 $m^2$ to about 1 $m^2$. After four tidal cycles, the currents reversed to an offshore direction, indicating undertow without any significant change in incident wave forcing (Figure 5). This negative morphodynamic feedback was probably due to the decrease in trough cross-sectional area, and it caused the formation of a new bar further seaward (AAGAARD, NIELSEN, and GREENWOOD, 1998). During the final two tidal cycles, only a single, isolated example of onshore-directed mean currents was recorded (at low tide with a small onshore discharge).

### SK00

The data selected from SK00 span three tidal cycles. The wave energy level was generally high with significant offshore wave heights up to 2.87 m and wave periods of 9–10 seconds. Measured and estimated hydrodynamic parameters at the inner bar crest (S3; see Figure 3) are illustrated in Figure 6. Wave heights decreased from the first to the second tidal cycle and then increased again from the second to the third cycle. Computed onshore discharge was generally three to five times larger than during SK95. Mean currents were consistently offshore-directed across the bar throughout the period, indicating undertow with maximum speeds of 0.3–0.4 m/s at high tide. As a consequence of the strong undertow, sediment was transported offshore, which caused trough erosion and seaward bar migration; consequently, $A_t$ increased significantly during the last two tidal cycles.

Undertow dominated the mean current circulation even though rip channels existed initially with a spacing of $\lambda = 290$ m. The main instrument transect crossed the subtidal bar midway between two such rip channels, which were active during instrument installation when low-energy conditions prevailed. Additional sensors were installed in rip and feeder channels (Figure 3). At the onset of the event, rip circulation was not evident; cross-shore flows were in fact larger at the bar crest and in the feeder channel ($U \approx -0.3$ m/s) than in the rip channel ($U \approx -0.2$ m/s) (Figure 7), perhaps because of the smaller water depths across the bar. However, the rip channel shoaled rapidly, and the sensor in the channel became buried; this infilling might have been caused by negative longshore sediment transport gradients because longshore current speeds decreased between the bar crest (S3) and the rip/feeder channels (Figure 7). Rip channels along the bar disappeared during the event, and the bar morphology became two-dimensional.

### SK02

This data set was obtained during three tidal cycles at the crest of an intertidal bar that was oblique to the shoreline. The experiment again demonstrated a switch from rip cell to undertow circulation. A rip channel was located 80 m downdrift, and another rip channel was approximately 95 m up-

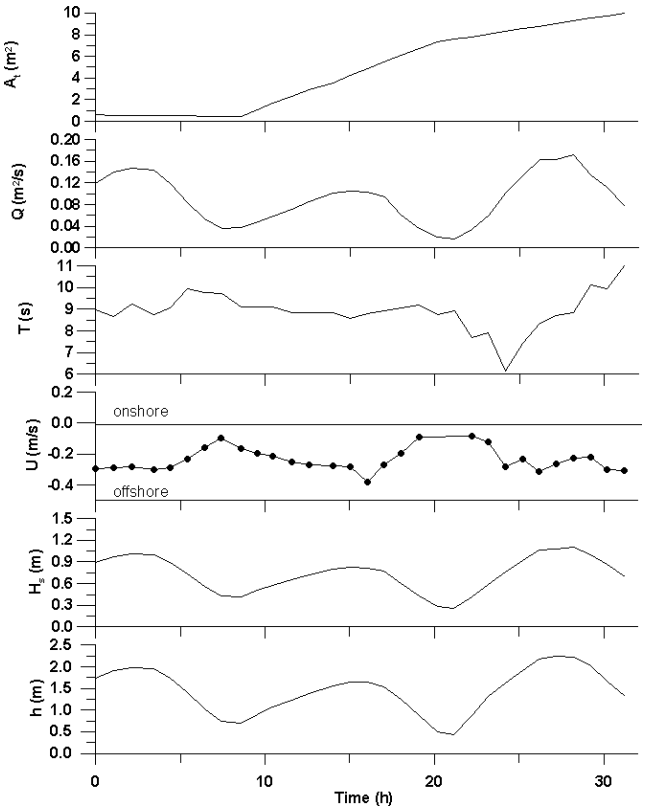


Figure 6. Hydrodynamic conditions at the inner bar crest during the SK00 experiment. The panels illustrate (bottom to top): mean water depth, significant wave height, and mean cross-shore current velocity, all at the crest of the inner bar; incident wave period at the seaward limit of the instrument array; calculated onshore discharge across the inner bar; and finally, cross-sectional area of the trough landward of the bar. Mean currents were consistently directed offshore.

drift of the instrument transect. Wave energy conditions were light to moderate; significant offshore wave heights increased from about 0.4 to 2.0 m, with wave periods of 6–7 seconds. Wave heights were small at the bar, where instruments were only inundated for short periods of time around high tide (Figure 8). Computed onshore discharge was small and comparable to the magnitudes obtained during SK95. Mean currents, which were recorded with an ADV at elevations of 2–3 cm above the bed, were less than 0.15 m/s and directed onshore during the first tidal cycle, consistent with visually observed active rip currents. Because of the onshore migration of the intertidal bar caused by the mean current, the trough cross-sectional area decreased from about 3 $m^2$ to 0 after two tidal cycles, when the bar merged completely with the beach. Consequently, at the beginning of the second tidal cycle, the mean current at the instrument position switched direction and flowed offshore. Thus, the morphological evolution and the morphodynamic feedbacks were similar to observations at SK95; an onshore bar migration caused a decrease in trough area and was associated with a switch from rip to undertow circulation.

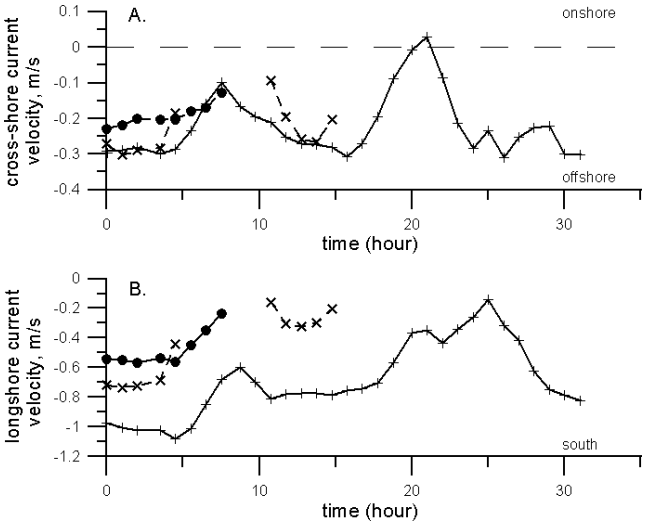


Figure 7. Cross-shore (A) and longshore (B) mean flows during the initial storm event at SK00. Currents were recorded at S3 (+), S8 (•), and S9 (×); see Figure 3 for instrument positions.

## EG02

During the EG02 experiment, data were recorded discontinuously over eight tidal cycles. Wave energy conditions increased during the period of data collection, which included a storm event with offshore significant wave heights up to 3.75 m with zero-crossing wave periods of about 7 seconds. Here, we use hydrodynamic data obtained at the crest of a longshore bar which had a crest level of approximately 0.2 m NAP (Dutch Ordnance Datum; see Figure 2). With normal wave conditions, the bar would have been classified as intertidal, but throughout the storm event, the bar was consistently inundated and active because of a small storm surge, and it clearly behaved as a subtidal bar. Rip channels existed 150 m either side of the instruments ($\lambda$ = 300 m); however, these channels were largely inactive and rip circulation during the periods of high wave energy were not visually observed. Inshore wave heights and onshore discharge were initially small but increased significantly during the storm period (Figure 9). Trough cross-sectional area was also small, although it did increase because of offshore bar migration during the storm. Mean currents were consistently directed offshore, indicating an undertow circulation, except for one record obtained at low tide.

## Circulation Type and Rip Channel Spacing

Calculated onshore mass transports are plotted against the ratio between trough cross-sectional area and distance from the instrument transect to the nearest rip channel ($A_t/y_r$; Figure 10). The data has been separated into cases with undertow and rip circulations, respectively. Undertow clearly preferably occurs for situations with large $Q$ and small ratios of $A_t/y_r$, and rip circulations occur for the opposite situation. To increase detail, Figure 11 plots the subset of the data with small magnitudes of $Q$. Here, it is evident that cases with

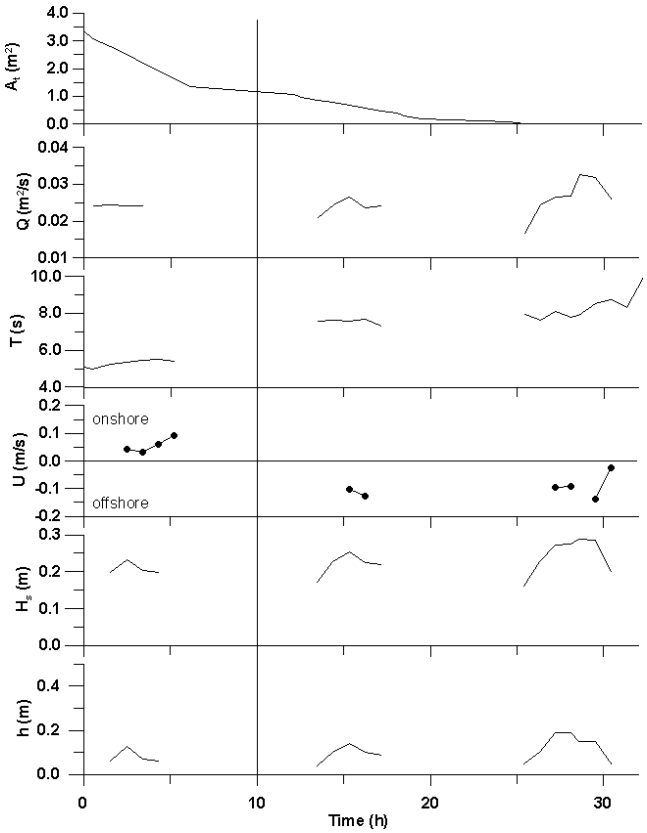


Figure 8. Hydrodynamic conditions at the inner (intertidal) bar crest during the SK02 experiment. The panels illustrate (bottom to top): mean water depth, significant wave height, and mean cross-shore current velocity, all at the crest of the bar; incident wave period at the seaward limit of the instrument array; calculated onshore discharge across the bar; and finally, cross-sectional area of the runnel landward of the bar. Waves were increasing; the first tidal cycle had onshore-directed mean current velocities (cell circulation), and the latter two had offshore-directed currents (undertows). The transition is marked by the vertical line.

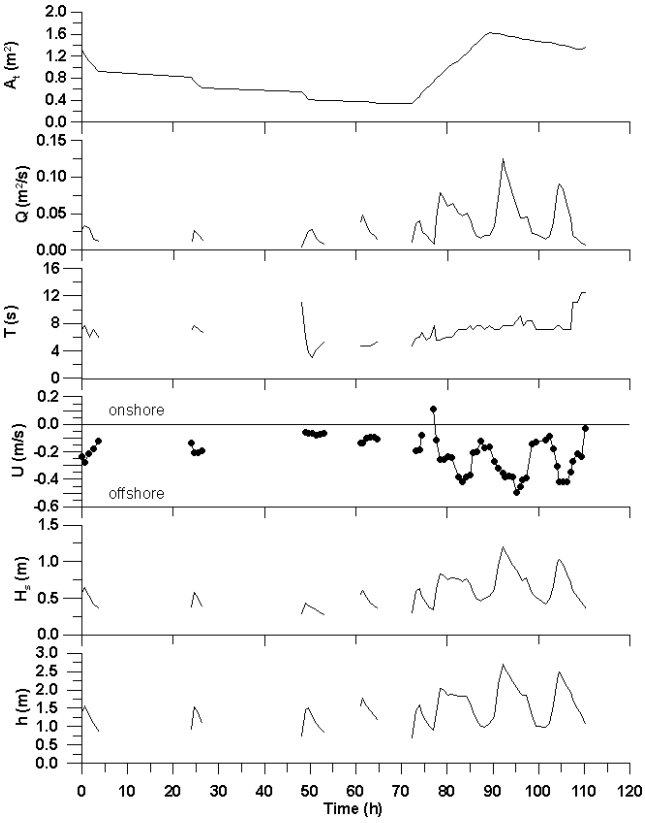


Figure 9. Hydrodynamic conditions at the inner bar crest during the EG02 experiment. The panels illustrate (bottom to top): mean water depth, significant wave height, mean cross-shore current velocity, incident wave period, calculated onshore discharge at the inner bar, and cross-sectional area of the trough landward of the bar. The eight tidal cycles had gradually increasing wave forcing and increasing water levels. Offshore-directed mean current velocities persisted throughout the records, except for one measurement of onshore-directed currents (hour 77).

either circulation type can be separated by a straight line through the data points; this line has a slope of approximately 1 (m/s).

Defining a morphodynamic unit as consisting of a longshore bar and the two rip channels at either end of this bar, an interesting corollary of the proposed relationships is that the maximum possible rip spacing ($\lambda = 2y_r$) for circulation cells involving the entire morphodynamic unit can be predicted. In Figure 11, the slope of the separation line is unity (m/s).

$$Q = \frac{A_t}{\lambda/2} \rightarrow \lambda = \frac{2A_t}{Q} \quad \text{(m)}. \tag{2}$$

For example, during SK95, the average trough area was initially on the order of 6 m$^2$, and a representative rate of onshore mass transport was 0.03 m$^3$ m$^{-1}$ s$^{-1}$ (Figure 5). For a cell circulation system spanning the entire morphodynamic unit, a maximum rip spacing of 400 m is predicted. The observed rip spacing at the beginning of the field experiment

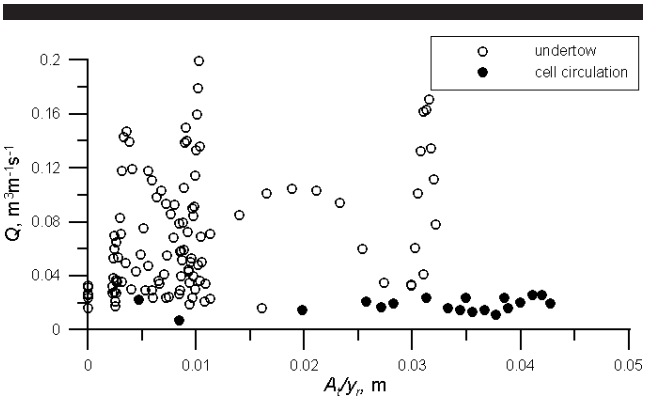


Figure 10. Scatter plot of all calculated onshore mass transport rates against $A_t/y_r$. Observations of rip current circulation are indicated by dots, and undertow cases are shown by open circles.

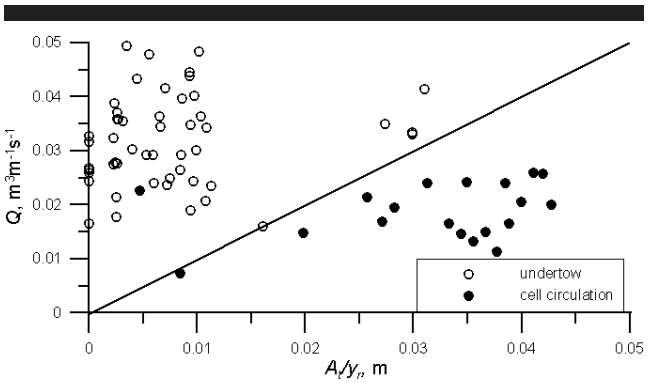


Figure 11. Same as Figure 10, but only including cases with onshore mass transport $<0.05$ m$^3$ m$^{-1}$ s$^{-1}$. The drawn line has a slope of 1 m/s and appears to separate the two types of cross-shore mean current circulation quite well.

was ~360 m. For the intertidal bar during SK02, the calculations yielded a maximum rip spacing of 260 m during the early stages of the experiment, whereas the measured active rip current/channel spacing was 250 m. The same calculation for the SK00 bar predicts a maximum spacing of 10 m increasing to 165 m, whereas the observed spacing was 290 m at the onset of the event. This indicates that with the given onshore discharge, trough area, the alongshore set-up gradient, or both were too small to generate a rip cell circulation (at least at the position of the instruments in the middle of the morphodynamic unit), and accordingly, an undertow was observed. At the undertow-dominated beach during EG02, the distance to the rip channel (150 m) was also probably too long to generate rip currents with the existing (small) trough area; the maximum range predicted with the model is $y_r$ = 30–65 m.

## DISCUSSION

The observations reported here suggest that nearshore circulation type depends on onshore discharge and trough geometry. For large wave heights (discharge) or small troughs and large rip channel spacings, or both, undertows are generated, whereas during more moderate energy conditions and larger troughs/shorter rip channel spacings, rip circulations occur. Hence, the occurrence of one type of circulation or another depends not only on forcing but also on prevailing morphology, as illustrated by the SK95 and SK02 experiments, in which circulation type changed without any significant change in energy conditions. The transition from rip to undertow was exclusively due to a morphodynamic feedback; with the given onshore discharge, the infilling of the trough caused by the landward bar migration inhibited rip current circulation. Our observations support the model proposed by DEIGAARD *et al.* (1999), who suggested that, for a given onshore discharge, an optimum relationship exists between $(A_t)^{1/2}$ and $\lambda$. If $\lambda$ is too large (or $A_t$ too small), longshore pressure gradients are too small to overcome frictional resistance in the trough. This inhibits rip feeder flow and generates an undertow circulation instead. Reversing the argument, for a given morphological configuration, relatively small onshore discharges result in rip circulation whereas a large onshore discharge can exceed trough drainage capacity. Note, however, that in contrast to DEIGAARD *et al.* (1999), we have used $A_t$ and not $(A_t)^{1/2}$ in the calculations.

The morphodynamic model proposed here (Figures 10 and 11) predicts rip cell flows for $Q < A_t/y_r$ and undertow circulations for $Q > A_t/y_r$. Hence, the slope of the line of data separation in Figure 11 is ~1 m/s. A physical interpretation of this dimensional number could be that it represents the maximum possible rip feeder velocity. When onshore discharge requires a current speed in the feeder channel in excess of 1 m/s, the hydraulic radius of the feeder channel might be too small to drain the volume of water; frictional resistance in the channel becomes too large and undertow is initiated. Coincidentally, maximum recorded rip current velocities are on the order of 1 m/s (MACMAHAN, THORNTON, and RENIERS, 2006).

Examining Figures 5 and 6, a strong relationship between circulation type and water depth across the bar crest appears to exist, with rip circulation occurring for relatively small water depths and undertow for relatively large depths. This is because of the nonlinear relationship between $Q$ and $h$. In Equation (1), $Q$ scales with the square of the wave height, which is depth-dependent (saturated) within the surf zone (*e.g.,* THORNTON and GUZA, 1989). Additionally, the wave phase velocity scales with the square root of $h$. Hence, the relationship between circulation type and $h$ is more apparent than real, with $Q$ being the controlling variable.

During the experiments, measurements were conducted mainly at bar crests, approximately midway between two rip channels (or in rip channels), and one of the main criteria for distinguishing between undertow and rip circulation was the direction of the mean flow across this bar crest. Measurements of active rip currents are not included in the data set. Such rip currents were recorded during an earlier experiment at Skallingen with a spacing of $\lambda \approx 900$ m (AAGAARD, GREENWOOD, and NIELSEN, 1997). Unfortunately, however, trough geometry away from rip channels was only surveyed approximately 2 weeks before and 2 weeks after an event when rip currents were active. The recorded rip current velocities were 0.15–0.60 m/s, and estimated onshore discharge was 0.05–0.12 m$^3$ m$^{-1}$ s$^{-1}$ (AAGAARD, GREENWOOD, and NIELSEN, 1997). The use of surveys of trough cross-sectional area at locations away from rips before the event that generated the rip currents ($A_t$ = 36 m$^2$), an $A_t/y_r$ ratio of 0.08 is obtained, Hence, a tentative estimate of $Q/(A_t/y_r)$ becomes 0.6–1.5 m/s, and the data points would have straddled the line of separation in Figures 10 and 11.

Because measurements were obtained approximately midway between two rip channels, the proposed model can predict whether the entire morphodynamic unit partakes in a rip cell circulation or not. It cannot predict, however, whether coexisting circulations occur, and it might be argued that cell circulation should always exist close to a rip channel. Such coexisting flows might not be likely, at least in an equilibrium situation in which hydrodynamics and morphology are coadjusted, for three reasons. First, to our knowledge, coexisting undertow and rip circulations within the same morphodyn-

amic unit have not been reported in the literature. Second, DEIGAARD *et al.* (1999) argued that a lower limit for the perturbation wavelength ($\lambda$) exists beyond which lateral mixing reduces the longshore pressure gradients required to drive the circulation. (In passing, we note that this lower limit has not been confirmed with the present data set.) Finally, measurements in a rip channel during rising wave conditions (Figure 7) revealed offshore-directed flows in the channel; flow magnitudes were approximately identical to, or lower than, flow magnitudes across the bar (*i.e.,* a rip current did not exist).

According to the model, existing rip channel spacings during the SK00 and EG02 experiments were too large for the given $Q$ and $A_t$. The question might be put why more closely spaced rip channels did not develop. It is possible that transient rip currents developed (away from instruments) without being observed and without creating rip channels. However, as wave heights and $A_t$ increased continuously (Figures 6 and 9), preferred rip spacings should continually change. Because of the significant hysteresis in nearshore morphodynamic systems (*e.g.,* COWELL and THOM, 1994), also with regard to rip channel position (*e.g.,* AAGAARD, GREENWOOD, and NIELSEN, 1997), it is probable that the system response was lagged; *i.e.,* rip channels did not have time to develop. Alternatively, the observations could indicate that minimum rip channel spacings do exist (*cf.* DEIGAARD *et al.,* 1999).

Morphological lags might also be the reason why the rip current observations in Figure 11 are not distributed along a straight line—for example, along the line of data separation. The lack of a straight line relationship could be due to the finite time it takes for the morphology to adjust to changing wave conditions because large amounts of sediment transport are involved in such adjustments.

Finally, it should be emphasised that the experiments were conducted on beaches with multiple quasi-linear to rhythmic bars, whereas transverse bar systems characterised by narrow, deeply incised rip channels and a lack of longshore troughs have not been studied. Such bar types frequently occur on single-barred beaches in swell-dominated settings (LIPPMAN and HOLMAN, 1990; MACMAHAN *et al.,* 2005; WRIGHT and SHORT, 1984). Hence, the results obtained are probably not valid for such bar systems.

## CONCLUSIONS

On the basis of four sets of field data from two different beaches, we propose a new approach to determine cross-shore mean current circulation type. The simple model predicts that the occurrence of rip currents or undertow depends on wave-induced mass transport rate across the bar ($Q$) and the geometry of the morphological system ($A_t/y_r$). For $Q/(A_t/y_r) > 1$, undertow occurs, whereas rip circulation is generated for $Q/(A_t/y_r) < 1$. The implication of this threshold is that when the mass transport of water across the longshore bar generates a longshore current velocity of more than about 1 m/s in the trough, the feeder channel becomes unable to drain the volume of water because frictional resistance exceeds the forcing by longshore pressure gradients and undertow is initiated. The opposite is the case when mass transport decreases so that the mean current velocity in the trough drops below 1 m/s. In this case, a transition from undertow to cell circulation may be initiated. Hence, the results obtained support the model proposed by DEIGAARD *et al.* (1999). Because the distance to the rip channel is included in the calculations, the maximum rip spacing can also be estimated from the model. Although the model does not address the physics of rip channel formation and the mechanisms determining the rip spacing, it does suggest that the nearshore system could be self-organizing.

## ACKNOWLEDGMENTS

We are grateful to Aart Kroon and the Rijkswaterstaat for helping out in the field experiment at Egmond. A large number of colleagues assisted in the Danish field experiments, including Jørgen Nielsen, Niels Nielsen, Brian Greenwood, Robin Davidson-Arnott, Michael Hughes, and Ulf Thomas. We appreciate the helpful suggestions by Rolf Deigaard, Aart Kroon, and an anonymous journal reviewer which led to significant improvements of the paper.

## LITERATURE CITED

AAGAARD, T., 2002. Modulation of surf zone processes on a barred beach due to changing water levels; Skallingen, Denmark. *Journal of Coastal Research,* 18, 25–38.

AAGAARD, T.; GREENWOOD, B., and NIELSEN, J., 1997. Mean currents and sediment transport in a rip channel. *Marine Geology,* 140, 25–45.

AAGAARD, T.; NIELSEN, J., and GREENWOOD, B., 1998. Suspended sediment transport and nearshore bar formation on a shallow intermediate-state beach. *Marine Geology,* 148, 203–225.

AAGAARD, T.; HUGHES, M.; SØRENSEN, R.M., and ANDERSEN, S., 2005. Hydrodynamics and sediment fluxes across an onshore migrating intertidal bar. *Journal of Coastal Research,* 22, 247–259.

AARNINKHOF, S.G.J.; TURNER, I.L.; DRONKERS, T.D.T.; CALJOUW, M., and NIPIUS, L., 2003. A video-based technique for mapping intertidal beach bathymetry. *Coastal Engineering,* 49, 275–289.

BOWEN, A.J., 1969. Rip currents. I. Theoretical investigations. *Journal of Geophysical Research,* 74, 5467–5478.

BOWMAN, D.; ARAD, D.; ROSEN, D.S.; KIT, E.; GOLDBERY, R., and SLAVICZ, A., 1988. Flow characteristics along the rip current system under low energy conditions. *Marine Geology,* 82, 149–167.

BRANDER, R.W., 1999. Field observations on the morphodynamic evolution of a low-energy rip current system. *Marine Geology,* 157, 199–217.

BRANDER, R.W. and SHORT, A.D., 2000. Morphodynamics of a large-scale rip current system at Muriwai Beach, New Zealand. *Marine Geology,* 165, 27–39.

COWELL, P.J. and THOM, B.G., 1994. Morphodynamics of coastal evolution. *In:* CARTER, R.W.G., and WOODROFFE, C.D. (eds.), *Coastal Evolution.* Cambridge, UK: Cambridge University Press, pp. 33–86.

DAMGAARD, J.; DODD, N.; HALL, L., and CHESTER, T., 2002. Morphodynamic modelling of rip channel growth. *Coastal Engineering,* 45, 199–221.

DAVIS, R.A. and HAYES, M.O., 1984. What is a wave-dominated coast? *Marine Geology,* 60, 313–329.

DEIGAARD, R.; DRØNEN, N.; FREDSØE, J.; JENSEN, J.H., and JØRGENSEN, M.P., 1999. A morphological stability analysis for a long straight barred coast. *Coastal Engineering,* 36, 171–195.

DRØNEN, N.; KARUNARATHNA, H.; FREDSØE, J.; SUMER, M.B., and DEIGAARD, R., 2002. An experimental study of rip channel flow. *Coastal Engineering,* 45, 223–238.

DYHR-NIELSEN, M. and SØRENSEN, T., 1970. Some sand transport phenomena on coasts with bars. *In: Proceedings 12th International*

*Conference on Coastal Engineering* (New York, ASCE), pp. 855–866.

FALQUES, A.; MONTOTO, A., and IRANZO, V., 1996. Bed-flow instability of the longshore current. *Continental Shelf Research,* 16, 1927–1964.

FREDSØE, J. and DEIGAARD, R., 1992. *Mechanics of Coastal Sediment Transport.* Singapore: World Scientific, 369p.

GARCEZ-FARIA, A.F.; THORNTON, E.B.; LIPPMANN, T.C., and STANTON, T.P., 2000. Undertow over a barred beach. *Journal of Geophysical Research,* 105(C7), 16999–17010.

GRANT, D.T., 1999. Wave-driven circulation on a barred beach and a beach with uniform longshore bathymetry. Hamilton, New Zealand: Department of Earth Science, University of Waikato. Master's thesis.

GREENWOOD, B. and OSBORNE, P.D., 1990. Vertical and horizontal structure in cross-shore flows: an example of undertow and wave set-up on a barred beach. *Coastal Engineering,* 14, 543–580.

GUZA, R.T.; CLIFTON, M.C., and REZVANI, F., 1988. Field intercomparisons of electromagnetic current meters. *Journal of Geophysical Research,* 93, 9302–9314.

HAAS, K.A.; SVENDSEN, I.A.; BRANDER, R.W., and NIELSEN, P., 2003. Modelling of a rip current system on Moreton Island, Australia. *In: Proceedings 28th International Conference on Coastal Engineering 2002* (New York, ASCE), pp. 784–796.

HAINES, J.W. and SALLENGER, A.H., 1994. Vertical structure of mean cross-shore currents across a barred surf zone. *Journal of Geophysical Research,* 99, 14223–14242.

HALLER, M.C.; DALRYMPLE, R.A., and SVENDSEN, I.A., 2002. Experimental study of nearshore dynamics on a barred beach with rip channels. *Journal of Geophysical Research,* 107, C6.

HOLMAN, R. and SALLENGER, A.H., 1993. Sand bar generation: a discussion of the Duck experimental series. *Journal of Coastal Research,* SI15, 76–92.

HOLMAN, R.A.; SYMONDS, G.; THORNTON, E.B., and RANASINGHE, R., 2006. Rip spacing and persistence on an embayed beach. *Journal of Geophysical Research,* 111, C01006.

HUNTLEY, D.A. and SHORT, A.D., 1992. On the spacing between observed rip currents. *Coastal Engineering,* 17, 211–225.

KLEIN, M.D. and SCHUTTELAARS, H.M., 2005. Morphodynamic instabilities of planar beaches: sensitivity to parameter values and process formulations. *Journal of Geophysical Research,* 110, F04S18.

KOMAR, P.D., 1998. *Beach Processes and Sedimentation,* 2nd edition. Upper Saddle River, New Jersey: Prentice-Hall, 544p.

KROON, A. and DEBOER, A., 2001. Horizontal flow circulation on a mixed energy beach. *In: Proceedings Coastal Dynamics 2001* (New York, ASCE), pp. 548–557.

KROON, A.; KRUIF, A.C.; QUARTEL, S., and REINTJES, C.M., 2003. Influence of storms on the sequential behaviour of bars and rips. *In: Proceedings Coastal Sediments 2003* (New York, ASCE), pp. 1–11.

LIPPMAN, T.C. and HOLMAN, R.A., 1990. The spatial and temporal variability of sand bar morphology. *Journal of Geophysical Research,* 95, 11575–11590.

LONGO, S.; PETTI, M., and LOSADA, I., 2002. Turbulence in the swash and surf zones, a review. *Coastal Engineering,* 45, 129–147.

MACMAHAN, J.; THORNTON, E.B., and RENIERS, A.J.H.M., 2006. Rip current review. *Coastal Engineering,* 53, 191–208.

MACMAHAN, J.; THORNTON, E.B.; STANTON, T.P., and RENIERS, A.J.H.M., 2005. RIPEX—rip currents on a shore-connected shoal beach. *Marine Geology,* 218, 113–134.

MASSELINK, G. and BLACK, K.P., 1995. Magnitude and cross-shore distribution of bed return flow measured on natural beaches. *Coastal Engineering,* 25, 165–190.

MCKENZIE, P., 1958. Rip current systems. *Journal of Geology,* 66, 103–113.

SHEPARD, F.P. and INMAN, D.L., 1950. Nearshore circulation. *In: Proceedings of the 1st Coastal Engineering Conference* (New York, ASCE), pp. 50–59.

SHORT, A.D., 1985. Rip current type, spacing and persistence, Narrabeen beach, Australia. *Marine Geology,* 65, 47–71.

SHORT, A.D. and HOGAN, C.L., 1994. Rip current and beach hazards: their impact on public safety and implications for coastal management. *Journal of Coastal Research,* Special Issue No. 12, pp. 197–209.

SONU, C.J., 1972. Field observation of nearshore circulation and meandering currents. *Journal of Geophysical Research,* 77, 3232–3247.

SVENDSEN, I.A., 1984. Mass flux and undertow in the surf zone. *Coastal Engineering,* 8, 347–365.

SVENDSEN, I.A., 1987. Analysis of surf zone turbulence. *Journal of Geophysical Research,* 92, 5115–5124.

THORNTON, E.B. and GUZA, R.T., 1989. Wind wave transformation. *In:* SEYMOUR, R.J. (ed.), *Nearshore Sediment Transport.* New York: Plenum Press, pp. 137–171.

WRIGHT, L.D. and SHORT, A.D., 1984. Morphodynamic variability of surf zones and beaches: a synthesis. *Marine Geology,* 56, 93–118.